Mineralogical Magazine, April 1998, Vol. 62(2), pp. 165–178

Leucite-pollucite structure-type variability and the structure of a synthetic end-member calcium wairakite ($CaAl_2Si_4O_{12}\cdot 2H_2O$)

C. M. B. HENDERSON

Department of Earth Sciences, University of Manchester, Manchester M13 9PL, and Daresbury Laboratory, Warrington WA4 4AD

A. M. T. BELL[1]

Daresbury Laboratory, Warrington WA4 4AD

S. C. KOHN[2]

Department of Physics, University of Warwick, Coventry CV4 7AL

AND

C. S. PAGE[3]

Department of Physics, King's College, University of London, London WC2R 2LS, UK

ABSTRACT

The structure of a synthetic end-member wairakite ($CaAl_2Si_4O_{12}\cdot 2H_2O$) has been determined using Rietveld analysis of high-resolution, synchrotron X-ray powder diffraction data, and ^{29}Si and ^{27}Al magic angle spinning nuclear magnetic resonance spectroscopy. The framework in the synthetic sample is more disordered than that in natural wairakite. Ca is distributed over the cavity cation sites M2, M12A, M12B in the approximate proportions 0.8:0.1:0.1, respectively, with M11 being vacant. ^{29}Si MAS NMR data are consistent with about 80% of the Si occupying tetrahedral T11 and T12 sites linked to two Al atoms [Q^4(2Al) silicons]. Tetrahedral and cavity cation site disorder are coupled so that Al mainly occupies T2 sites, with Ca in M12A and M12B being balanced by Al in T12A and T12B; T11A and T11B sites appear to only contain Si, in agreement with the M11 site being vacant. The crystal chemistries of the wide range of stoichiometries which crystallize with the leucite/pollucite structure-type are also reviewed, with particular attention being paid to the tetrahedral ordering configurations present in these phases, and the implications to crystallographic phase transitions.

KEYWORDS: wairakite, leucite, pollucite, Rietveld analysis, crystal structure.

Introduction

SILICATES with three-dimensional tetrahedral framework structures form a wide range of distinct structure types, with many representatives amongst the rock-forming minerals (e.g. silica minerals, feldspars, nepheline, leucite, sodalite, zeolites). Studies of synthetic structural analogues, many of which are distinctive in that they have rare elements substituting for the more abundant elements, have greatly aided in understanding the detailed structural behaviour of the natural minerals (Taylor, 1983; 1984; Henderson,

Now at:
[1] Department of Chemistry, University of Cambridge, Lensfield Road, Cambridge CB2 1EW
[2] Department of Geology, University of Bristol, Bristol BS8 1RJ
[3] Department of Chemistry, Imperial College of Science, Technology and Medicine, University of London, London SW7 2AY

1984; Torres-Martinez and West, 1989; Palmer *et al.*, 1997). From a crystal chemical point of view, such analogues allow studies to be carried out on how different chemical species influence the ordering of tetrahedral cations and/or extra-framework (cavity) cations over distinct structural sites; such ordering may lead to the occurrence of very sluggish, reconstructive phase transitions between polymorphs.

As part of a wider attempt to understand the controls and consequences of atomic substitution and cation ordering in compounds with framework structures, we are studying a series of synthetic silicates with structures related to those of the natural minerals leucite, pollucite and analcime. Another mineral with the leucite-type topology is wairakite, the analogue of analcime in which two cavity Na^+ cations are replaced by one Ca^{2+} coupled with Si-Al ordering (Coombs, 1955; Takéuchi *et al.*, 1979). Natural wairakite contains a significant Na content complicating the ordering pattern to some degree. In this paper we review the chemical and structural variation of the leucite structure type, and describe the structure of synthetic Ca end-member wairakite, Our new work on wairakite is based on the application of high-resolution, synchrotron powder diffraction, and of ^{29}Si and ^{27}Al magic angle spinning, nuclear magnetic resonance spectroscopic methods.

Variable stoichiometries in the leucite structure type

The mineral leucite ($KAlSi_2O_6$) has a structure consisting of a three-dimensional framework of $(Al,Si)O_4$ tetrahedra. The ideal formulae for the natural structural analogues are: analcime $NaAlSi_2O_6{\cdot}H_2O$, pollucite $CsAlSi_2O_6$, and wairakite $CaAl_2Si_4O_{12}{\cdot}2H_2O$; note the presence of molecular water in analcime and wairakite. The aluminosilicate framework contains two sizes of channels, the larger occupied by K in leucite, Cs in pollucite and H_2O in analcime and wairakite, and the smaller by Na in analcime and Ca in wairakite (Mazzi *et al.*, 1976; Galli *et al.*, 1978).

At room temperature and pressure, pollucite is cubic with space group *Ia3d*, analcime is cubic *Ia3d* (or pseudo-cubic: tetragonal $I4_1/acd$, orthorhombic *Ibca*, Mazzi and Galli, 1978; monoclinic *I2/a*, Pechar, 1988), while K-leucite has a distorted structure having the tetragonal space group $I4_1/a$. With increasing temperature, the low-temperature, tetragonal structure in K-leucite shows a continuous, rapid (non-quenchable), displacive transition to the high-temperature form (*Ia3d*; Peacor, 1968; Taylor and Henderson, 1968), perhaps via intermediate phases (Faust, 1963; Lange *et al.*, 1986; Palmer *et al.*, 1989). In this context, note that there is only a single T site in *Ia3d*, indicating that Al and Si must be disordered if high-leucite belongs to this space group. This in turn indicates that tetragonal low-leucite ($I4_1/a$) should also have Si and Al disordered over the three T-sites, as the phase transition is too rapid to allow the possibility of Al-Si ordering. However, the situation is much more complex than this because MAS NMR for natural, $I4_1/a$ K-leucites demonstrates partial Si-Al ordering, although there is controversy regarding the ordering scheme over the three T sites (e.g. Murdoch *et al.*, 1988; Phillips *et al.*, 1989; Kohn *et al.*, 1995; Kohn *et al.*, 1997). Clearly, such partially ordered frameworks could not transform to *Ia3d* symmetry, even though the lattice becomes metrically cubic above the phase transition (Palmer *et al.*, 1989).

In addition to the variations shown by Al-Si analogues, the leucite-type structure shows a wide variety of substitutions involving both tetrahedral and cavity sites. As well as K, Cs, Na and Ca occurring as cavity cation species, Rb (Henderson and Taylor, 1969; Palmer *et al.*, 1997) and Tl^+(Henderson and Taylor, 1969) varieties have been synthesized. In particular, the tetrahedral framework can readily accommodate a wide range of multivalent substitutions including univalent (e.g. Li) and divalent (e.g. Be, Mg, Fe, Zn, Cd, Co, Cu) ions (e.g. Roedder, 1951; Bayer, 1973; Torres-Martinez and West, 1989; Taylor, 1991; Heinrich and Baerlocher, 1991; Kohn *et al.*, 1994; England *et al.*, 1994; Bell and Henderson, 1994*a*, 1996). Other trivalent (e.g. B, Fe, Cr, Ga) and tetravalent (Ge) cations can be substituted for Al and Si (e.g. Ohmsbredemann *et al.*, 1986; Torres-Martinez and West, 1989; Taylor, 1991; England *et al.* 1994; Bell and Henderson, 1994*b*); a P^{5+} end member is also known (Ren *et al.*, 1990). SiO_2-rich, alkali-deficient leucites can also be directly synthesized by hydrothermal methods leading to samples with cavity cation site vacancies (Henderson, 1969). The unit cell stoichiometries (anhydrous) of these 'end-members' can be expressed as follows:

Basic formula: (i) $X^+_{16}T^{3+}_{16}T^{4+}_{32}O_{96}$
(analcime, leucite, pollucite);

Variants: (ii) $X^+_{16}T^+_{5.33}T^{4+}_{42.67}O_{96}$;

(iii) $X^{+}_{16}T^{2+}_{8}T^{4+}_{40}O_{96}$;

(iv) $X^{+}_{12}\square_{4}T^{3+}_{12}T^{4+}_{36}O_{96}$ (where $\square$ = vacancy);

(v) $X^{+}_{16}T^{3+}_{32}T^{5+}_{16}O_{96}$;

(vi) $X^{2+}_{8}T^{3+}_{16}T^{4+}_{32}O_{96}$ (wairakite)

In the case of the phases with divalent tetrahedral cations (stoichiometry (iii) above), polymorphs exist with different numbers of T sites and different tetrahedral ordering arrangements (Heinrich and Baerlocher, 1991; Kohn *et al.*, 1991, 1994; Bell *et al.*, 1994*a*, *b*). For example, at room temperature, $K_2MgSi_5O_{12}$ has been shown to be monoclinic $P2_1/c$ with a fully ordered framework consisting of 10 Si and 2 Mg sites (Bell *et al.*, 1994*a*) and $Cs_2CdSi_5O_{12}$ to be orthorhombic *Pbca* with 5 Si and 1 Mg sites (Bell *et al.*, 1994*b*). $P2_1/c$ is a maximal sub-group of *Pbca* (cf. $I4_1/a$ and *Ia3d* in the case of K-leucite) and Redfern and Henderson (1996) have recently shown that $P2_1/c$ $K_2MgSi_5O_{12}$ shows an unquenchable and reversible, first-order, ferroelastic phase transition to the *Pbca* structure at 350°C.

As well as the intrinsic interest in studying this varied structure type, its technological importance is reflected in recent work on aluminosilicate leucite-pollucites regarding their existing and potential uses in such areas as: fluid cracking catalysts (Kumar *et al.*, 1993); glass ceramics (e.g. Hogan and Risbud, 1991); radioactive waste disposal (e.g. Yanagisawa *et al.*, 1987); water purification (e.g. Nishioka *et al.*, 1990); dental porcelains (e.g. Mackert *et al.*, 1994); and as fast ion conductors (Palmer and Salje, 1990).

Structure of natural wairakite

Natural wairakite, first described by Steiner (1955), invariably contains small but significant amounts of Na replacing Ca in the ideal formula (typically 0.18–1.88 wt.% Na_2O; Aoki and Minato, 1980). Coombs (1955) carried out the first X-ray investigation and showed that it was a pseudo-cubic or pseudo-tetragonal variant of the analcime structure; he suggested that its real structure was monoclinic, either *Ia* or *I2/a*. Coombs (1955) also compared multiple twinning in wairakite to that shown by leucite and speculated that wairakite had originally crystallized as a cubic, analcime-like phase and had transformed to the low symmetry polymorph by a "non-reconstructive type of phase transformation" on cooling. Coombs suggested that the divalent Ca ions could be associated with two Al T-sites and thus inferred that wairakite had an ordered Si-Al arrangement.

Takéuchi *et al.* (1979) used single crystal X-ray methods to study a natural sample of composition $Ca_{7.19}Na_{1.12}K_{0.1}(Si_{32.59}Al_{15.38})O_{96}\cdot 16H_2O$, and confirmed that natural wairakite is monoclinic *I2/a* with a unit cell formula containing six distinct T sites (3 pairs of related sites) [T11A and T11B, T12A and T12B, T2A and T2B; each site of multiplicity 8] and four cavity cation sites (M11 and M2 each of multiplicity 8, and M12A and M12B, each of multiplicity 4). Based on T–O bond length differences, Takéuchi *et al.* showed that Si was dominantly ordered into T11A (93% Si), T11B (94%), T12A (95%), and T12B (95%) sites and Al into T2A (84%Al) and T2B (84%) sites. Note the same occupancy for each 'pair' of related T sites. Each T1(Si) site is linked to two T2(Al) and two T1(Si) sites and each T2(Al) is linked to four (T1Si) sites in accordance with the Al-avoidance principle (Loewenstein, 1954). The octahedral cavity cation M2 sites are linked to two oxygens each of adjacent Al-bearing T2A and T2B tetrahedra, and to the oxygens of two water molecules. Ca was placed in the M2 sites as close to Al as possible, in effect coupling the T-site ordering of Al to the M-site ordering of Ca so that the Al occupancy of Al in T2 effectively balances that of Ca in M2. The M-site occupancies were thus inferred to be M11 (4.2%Na, 95.8%$\square$ (vacancy)), M12A (3.4%Na, 96.6%$\square$), M12B (4.1%Na, 95.9%$\square$), M2 (89.9%Ca, 5.9%Na, 4.2%$\square$).

Experimental methods

Synthesis

The starting material was prepared by thoroughly mixing appropriate amounts of SPECPURE amorphous SiO_2, amorphous Al_2O_3 prepared by heating hydrated aluminium nitrate at 600°C, and SPECPURE $CaCO_3$; X-ray fluorescence analysis showed that the anhydrous Al_2O_3 contains less than 0.3wt.% Na_2O. The mixture was heated overnight at 600°C to decompose the carbonate; the product was amorphous to X-rays. About 0.5g of this mixture was sealed with excess water in a platinum tube and heated in a cold seal pressure vessel at 310°C and 2 kbars for 91 days. Using a laboratory X-ray diffractometer and Cu-K_α radiation, the wairakite showed a partially split 400/004 peak and the presence of a few

percent of each of quartz and anorthite as impurities. In addition, ^{27}Al MAS NMR showed that a small amount of an unidentified impurity phase with octahedrally coordinated Al was present. The synthetic wairakite was fine grained (mean grain size of 10–30 μm) necessitating the use of powder rather than single crystal methods for structure determination.

Powder dispersed on double sided sticky tape and carbon coated was analysed on a JEOL 6400 SEM fitted with a LINK XL system high efficiency 'Pentafet' energy dispersive detector at 15 keV, 1.5 na beam current, and a 5 μm raster. Standards used were synthetic corundum for Al and wollastonite for Si and Ca and data were reduced with LINK ZAF4 software. The mean values obtained for analyses of 5 grains (1σ in brackets) are SiO_2 57.1(1.3), Al_2O_3 23.7(1.0), CaO 13.3(0.5) wt.%; Fe and Na were below detection (<0.08%). The equivalent anhydrous formula is $Ca_{1.01}Al_{1.97}Si_{4.02}O_{12}$, within error of the stoichiometric end-member composition. The water content of the sample was determined in duplicate by thermogravimetric analysis giving a mean value of 8.13 wt.%, very close to the theoretical value of 8.28 wt.%.

Synchrotron X-ray powder diffraction

The very low divergence of synchrotron radiation and the availability of high resolution diffractometers, together with Rietveld peak deconvolution techniques, allows the determination of structural data for powdered samples. Thus synchrotron X-ray powder diffraction was used to determine the structure of synthetic end-member wairakite using station 2.3 at the Daresbury Laboratory (Cernik *et al.*, 1990; Collins *et al.*, 1992). The samples were loaded onto an aluminium flat plate container 25 mm in diameter and 1 mm deep. Data were collected at room temperature over the range of 5–80 degrees 2θ using monochromatic radiation (water cooled Si (111) monochromator) of wavelength 1.40285 Å (calibrated against NIST 640b silicon standard) using steps of 0.01°2θ and counting times of 2.5 seconds per step. Each peak consists of overlapping reflections and the best estimate of peak width at half height is about 0.07°2θ showing that the sample is reasonably well crystalline despite the low synthesis temperature.

The structure was refined by the Rietveld method (Rietveld, 1969) using MPROF in the Powder Diffraction Program Library (Murray *et al.*, 1990); only data in the range 5–70° 2θ (2307 peaks) were used as the signal:noise ratio higher than 70° 2θ does not allow adequate deconvolution of the very large number of low intensity, overlapping peaks in this region (Fig. 1). Refinements were carried out using neutral atom X-ray scattering factors (International Tables, volume IV, Table 2.3.1) and, because of the close similarity between those for Si and Al, T-site disorder was assumed (i.e., 1/3Al, 2/3Si on each site). The structural model was based on the results for natural wairakite, *I2/a* (Takéuchi *et al.*, 1979). In the first stage of the refinement, all the T–O distances were constrained to have a value of 1.67 ± 0.02 Å. After the Rietveld refinement converged, the constraints were changed so that all T–O distances in a given tetrahedron were constrained, but T–O distances in different tetrahedra were allowed to vary. As is normal in X-ray methods, the mean refined T–O bond length for each distinct tetrahedral site can be used to infer the Si-Al occupancy for that site. During the final stages of the data reduction, the occupancies of the Ca sites and the isotropic temperature factors (B) were refined. Note that all Ca-, all T-, and all O-sites were constrained to have the same B values.

Because of the presence of anorthite and quartz as minor impurities, a three-phase Rietveld refinement was carried out using the structural parameters of Jorgensen (1978) for quartz and of Bruno *et al.* (1976) for anorthite. The final refinement gave the statistical parameters: R_I 8.2, R_{WP} 14.2 %; R_{exp} 10.9%; and goodness of fit 1.71. The errors in the structural parameters are relatively large due to the inherent problem of using powder diffraction methods to determine the structures of weakly scattering, low-symmetry materials which show only limited distortions from cubic/tetragonal symmetry. Thus the number of independent parameters to be refined was kept as small as possible because we found that more complicated structural models (e.g. taking account of T-site ordering, and entry of Ca onto the M11 site) tended to give unrealistic values for individual bond lengths and angles, which in turn distorted the mean values which we use to discuss the overall structural relations. Figure 1 shows the experimental diffraction data, the calculated positions of all possible reflections, and the plot of the differences between the experimental and calculated intensities.

MAS NMR

This technique is complementary to X-ray diffraction in that element-specific, short-range

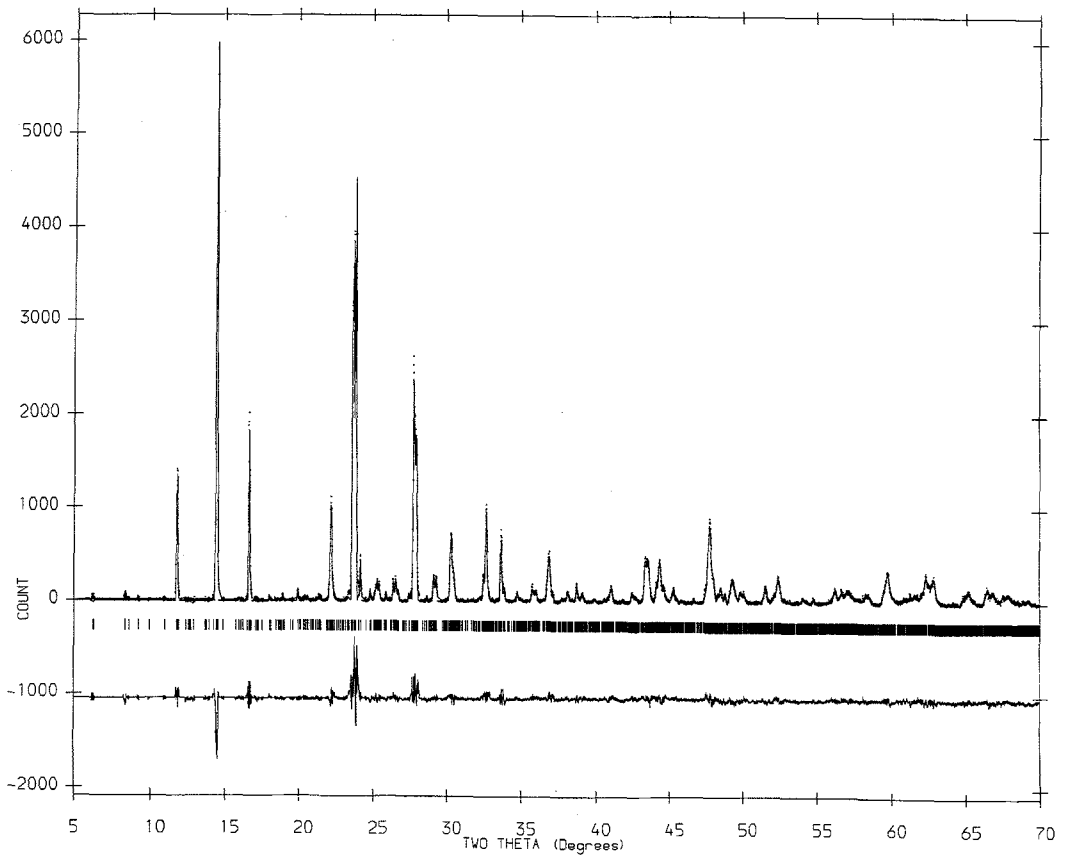

FIG. 1. High-resolution powder diffraction pattern of end-member wairakite. The upper panel shows the experimental data (spots) and calculated pattern (solid line) for the refined structure. The middle panel shows the positions of all possible reflections and the lower panel shows the difference plot $[(I_{obs} - I_{calc})/\sigma_{obs}]$ between the experimental and calculated patterns.

order information can be obtained for both Si and Al independently, allowing inferences to be made regarding the ordering of these cations into distinct structural sites. ^{29}Si NMR spectra were obtained using a Bruker MSL 360 spectrometer operating at 71.535 MHz. It was found that ^{29}Si in the sample had a very long spin relaxation time (T1) therefore long recycle delays were required. The ^{29}Si data obtained consists of the addition of 48 pulses with a 60 minute recycle decay and 92 pulses with a 30 minute delay, i.e. a total acquisition time of 94 hours. The pulse width was 2 μs ($\sim \pi/6$), the dwell time was 40 μs, and the spinning speed 2.93 kHz. ^{27}Al spectra were obtained at two magnetic fields, 14.1 T and 8.45 T using a Varian VXR 600 and the MXL 360 spectrometers, respectively. Pulse lengths of 3 μs (high field) and 1 μs (low field), and recycle delays of 0.5 s were used.

Results and discussion

X-ray diffraction

The synchrotron diffraction data for synthetic wairakite show a clear splitting of the pseudo-cubic {400} peaks at about 24°2θ (Fig. 1). Thirty peaks between 10 and 40° 2θ provide the cell parameters a = 13.694(6), b = 13.644(7), c = 13.576(6) Å, β = 90.46(2)°; these values compare with those for natural wairakite (Takéuchi *et al.*, 1979) of 13.692(3), 13.643(3), 13.560(3), 90.5(1), respectively. The difference between the c axes

for the two samples leads to c/a ratios of 0.9916(6) and 0.9904(3), respectively, which are different at the 1σ level. Thus the synthetic sample is slightly less distorted from the cubic pseudo-cell than the natural sample. Refined fractional atomic coordinates are given in Table 1, and mean T–O and Ca–O bond lengths, and mean T–O–T bond angles for the different T sites are summarised in Table 2. Tetrahedral and cavity cation connectivities are summarized in Table 3 (after Takéuchi *et al.*, 1979).

Initially the refinement was carried out with 'pairs' of T-sites (T11A and T11B; T12A and T12B; and T2A and T2B) constrained to give similar T–O bond lengths which gave the results: T11A–O 1.63, T11B–O 1.63, T12A–O 1.67, T12B–O 1.66, T2A–O 1.70, T2B–O 1.73 Å for mean bond lengths. These values suggest that T11 sites are mainly occupied by Si, T2 by Al , and with significant Al in T12 sites. In subsequent refinements the T-sites were allowed to refine independently with the surprising result that the T12A–O and T12B–O bond lengths diverged. The final mean T–O bond lengths (in angstroms) for each tetrahedron, (compared with those from Takéuchi *et al.* in parentheses), are T11A–O 1.63 (1.609), T11B–O 1.63 (1.616), T12A–O 1.66 (1.612), T12B–O 1.61 (1.612), T2A–O 1.74 (1.726) and T2B–O 1.71 (1.732). Bearing in mind that the standard deviations of the individual T–O bond lengths in our powder refinement are ~ 0.02 Å, these mean T–O values are in reasonable agreement except that the T12A tetrahedron bond lengths appear to be significantly longer for our sample. Our bond lengths for T11-type and T12B tetrahedra are close to the mean Si–O for anorthite and low albite of 1.615 Å, and those for T2 type tetrahedra are similar to the mean Al–O of 1.745 Å in these ordered feldspars; the

TABLE 1. Fractional atomic coordinates, isotropic temperature factors and Ca-site occupancies for synthetic end-member wairakite

Atom	X	Y	Z	B(iso)	Occupancy
Ca12A	0.2500	0.127(3)	0.0000	2.9(2)	0.97(3)
Ca12B	0.7500	0.385(3)	0.0000	2.9(2)	0.79(4)
Ca2	0.011(1)*	0.248(1)	0.118(1)	2.9(2)	6.24(5)
T11A	0.117(1)	0.155(1)	0.419(1)	0.29(7)	
T11B	0.877(1)	0.341(1)	0.407(1)	0.29(7)	
T12A	0.423(1)	0.130(1)	0.153(1)	0.29(7)	
T12B	0.591(1)	0.367(1)	0.164(1)	0.29(7)	
T2A	0.170(1)	0.416(1)	0.139(1)	0.29(7)	
T2B	0.844(1)	0.088(1)	0.119(1)	0.29(7)	
O11A	0.110(1)	0.350(2)	0.231(1)	0.32(9)	
O11B	0.907(1)	0.138(2)	0.217(1)	0.32(9)	
O12A	0.385(1)	0.138(2)	0.462(1)	0.32(9)	
O12B	0.599(1)	0.355(1)	0.477(1)	0.32(9)	
O21A	0.208(1)	0.116(2)	0.352(1)	0.32(9)	
O21B	0.777(1)	0.394(2)	0.374(1)	0.32(9)	
O22A	0.128(1)	0.466(1)	0.397(1)	0.32(9)	
O22B	0.834(1)	0.045(1)	0.362(1)	0.32(9)	
O31A	0.387(1)	0.224(1)	0.084(1)	0.32(9)	
O31B	0.645(1)	0.277(1)	0.112(1)	0.32(9)	
O32A	0.477(1)	0.385(2)	0.141(1)	0.32(9)	
O32B	0.545(1)	0.111(1)	0.170(1	0.32(9)	
W A	0.137(1)	0.116(2)	0.134(1)	0.32(9)	
W B	0.880(1)	0.381(2)	0.112(1)	0.32(9)	

Cell parameters: a 13.694(6), b 13.644(7), c 13.576(6) Å, β 90.46(2)
Structure fit parameters: R_I 8.2; R_{WP} 14.2%; R_{exp} 10.9%; goodness of fit 1.71
* One sigma errors in brackets

TABLE 2. Mean tetrahedral (T) and cavity cation (M) bond lengths, and mean inter-tetrahedral (T–O–T) angles for synthetic wairakite.

Mean bond lengths (Å)		Mean T–O–T angles (°) for each T site	This work	Takéuchi *et al.* (1979)
T11A–O	1.63(2)	T11A	144.3(2.0)	147.4(2.5)
T11B–O	1.63(2)	T11B	136.3(11.7)	139.9(8.5)
T12A–O	1.66(3)	T12A	136.5(10.1)	141.6(7.6)
T12B–O	1.61(2)	T12B	140.3(3.4)	141.9(9.1)
T2A–O	1.74(2)	T2A	141.3(4.3)	145.0(6.3)
T2B–O	1.71(2)	T2B	143.5(7.8)	140.2(11.6)
M12A–O	2.49(8)			
M12B–O	2.44(11)			
M2–O	2.47(6)			

T–O bond lengths for the T12A tetrahedra is intermediate. Based on these data, and by analogy with the work of Takéuchi *et al.*, we conclude that Si in synthetic wairakite is mainly ordered into T11 and Al into T2 sites. Based on mean T–O distances, the T12B site is occupied by Si while the T12A appears to contain a significant amount of Al; this difference is unexpected bearing in mind that these two sites are a crystallographic 'pair' with the same connectivities (Table 3). In this context note that the single crystal data (Takeuchi *et al.*, 1979) indicate that the bond lengths for T12A and T12B are identical.

Projections of the structure perpendicular to the *b* axis [010] and perpendicular to <111> are shown in Fig. 2. Note that two types of four-rings of tetrahedra occur in the [010] plane, namely T11A-T2A-T11A-T2A and T11B-T2B-T11B-T2B, both with two pairs of the same species (Fig. 2*a*), while a four-ring with four different tetrahedral species, namely T11A-T12A-T11B-T12B occurs perpendicular to *c*, and similarly, four-rings containing T12A-T2A-T12B-T2B occur parallel to [100]. Figure 2*a* shows the symmetrical equivalence of the T11A and T11B, T12A and T12B, and T2A and T2B pairs of tetrahedra in the monoclinically distorted pseudo-orthorhombic cell (Takéuchi *et al.*, 1979).

In the initial refinements, Ca was placed exclusively on the M2 cation site, the site occupied

TABLE 3. Tetrahedral (T)- and cavity cation (M)-site connectivities

Site	T11A	T11B	T12A	T12B	T2A	T2B
T11A	–	–	1	1	2	–
T11B	–	–	1	1	–	2
T12A	1	1	–	–	1	1
T12B	1	1	–	–	1	1
T2A	2	–	1	1	–	–
T2B	–	2	1	1	–	–
M11*	1	1	–	–	–	–
M12A	–	–	2	–	–	–
M12B	–	–	–	2	–	–
M2	–	–	–	–	1	1

* Ca is coordinated by 6 oxygens; two oxygens on each of the two tetrahedra shown, plus 2 waters.

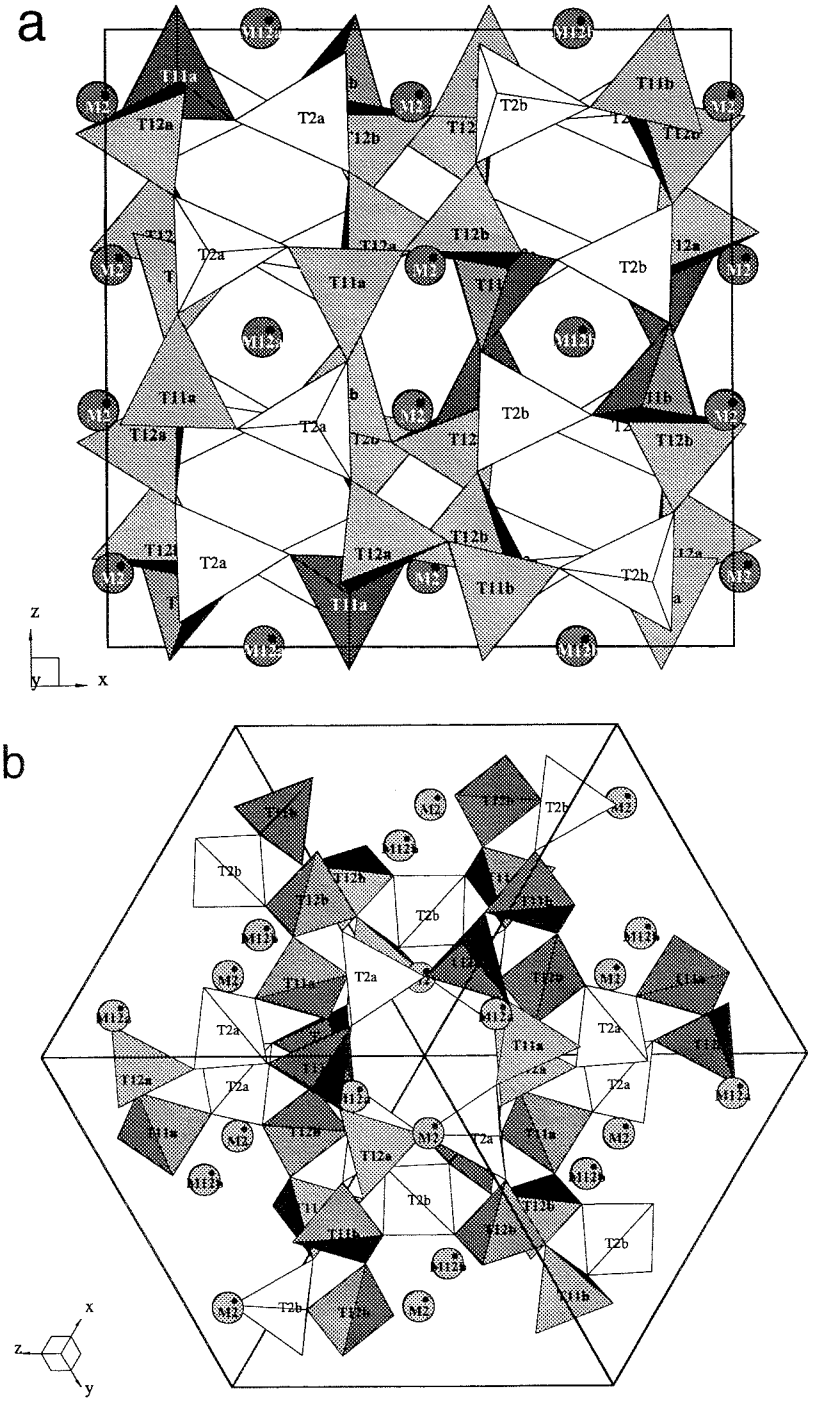

FIG. 2. Projected structures of synthetic Ca-wairakite: (a) Perpendicular to the *b* axis, [010] plane; (b) Perpendicular to <111>. Shaded tetrahedra are those occupied mainly by Si, and unshaded tetrahedra mainly by Al. The positions of water molecules and of the vacant M11 sites are not shown.

by all the Ca in the structural refinement of Takéuchi *et al.* (1979). However in later refinements, we allowed Ca to disorder between the different cavity cation sites. As shown in Table 1, Ca is mainly concentrated in M2 (~78% Ca) but significant and similar amounts seem to enter the M12A (~12% Ca) and M12B (~10% Ca) 'pair' of cation sites. Although earlier refinements suggested the presence of minor Ca on M11, the Ca–O distance was not structurally sensible so this site was left vacant in later refinements. Figure 2*a* shows the positions of the M12A, M12B, and M2 Ca sites; note the symmetrically equivalent M12A and M12B pair of Ca sites. The projection in the [111] plane (Fig. 2*b*) demonstrates that the large W sites, located at the centre of the projection, are not occupied by Ca.

The mean Ca–O bond lengths for the three different sites occupied are very similar (M12A–O 2.49, M12B–O 2.44, M2–O 2.47 Å) and very close to that for the 6-coordinated Ca site in anorthite (2.453 Å). Bearing in mind that Takéuchi *et al.* (1979) showed that the ordering of Ca into M2 is coupled to that of Al into T2-sites, it seems likely that the presence of significant amounts of Ca in M12-sites in synthetic Ca-wairakite should be accompanied by the presence of significant Al in the adjacent T-sites, while the T-sites adjacent to the vacant M11 site would be expected to be mainly occupied by Si. The connectivities associated with the cavity cation sites are shown in Table 3. M11 can be seen to share 2 oxygens with each of T11A and T11B, M12A is linked to 2 T12A, M12B is linked to 2 T12B, and M2 is coordinated to T2A and T2B. Thus based on the Ca occupancies obtained for each of the M sites: T11 sites should contain only Si (M11 vacant); substantial Ca contents in M12A and M12B imply the presence of significant amounts of Al in T12A and T12B, respectively; and the fact that the bulk of Ca occurs in the M2 site implies the presence of major Al in T2A and T2B. These predictions are in line with those based on mean T–O bond lengths except for the T12A site, which seems to have an anomalously short mean T–O distance of 1.61 Å. On balance, we believe that the similar Ca occupancies of M12A and M12B, which imply similar occupancies of Al in T12A and T12B, is the more reliable result. This relationship is in line with the fact that T12A and T12B are a 'pair' with the same connectivities, which have the same mean T–O bond lengths in the natural mineral single crystal structure obtained by Takéuchi *et al.* (1979), which is more reliable than our structure derived from powder methods.

The mean T–O–T angles for each T site calculated from our data for the Ca end-member wairakite are summarised in Table 2 together with equivalent data for the natural wairakite from Takéuchi *et al.* (1979). The order of increasing mean T–O–T angles for the sites occupied by Si are the same in both data sets, although the absolute values for each T-site-species show substantial differences. By contrast, the T–O–T angles for the sites occupied by Al (T2) are reversed in the two data sets. The errors in individual T–O–T angles in our data are 1–2°, so it is likely that the larger differences between the mean values are significant, and reflect the stoichiometric and ordering differences between the samples.

NMR spectroscopy

The ^{29}Si MAS NMR spectrum of synthetic wairakite is shown in Fig. 3 and consists of three peaks at around −94.0, −96.6, and −98.6 ppm, together with some small shoulders on both the shielded and de-shielded sides of the main peaks. The small peak at about 107 ppm is due to a quartz impurity (about 1–2%). Although the presence of anorthite was detected by X-ray diffraction, the main ^{29}Si peaks for anorthite at about −82 and −84 ppm (Phillips *et al.*, 1992) were not detected above the background (Fig. 3). The shifts for the three main ^{29}Si peaks are within the range observed for Si in $Q^4(2Al)$ sites, i.e. Si attached to two SiO_4 and two AlO_4 tetrahedra (−92 to −102 ppm, Kirkpatrick *et al.*, 1986). An approximate integration of the spectrum indicates that the proportions of the areas of the peaks are 2:1:1, with the −94.0 ppm peak having twice the area of the other two peaks. This is broadly consistent with the crystal structure data for synthetic wairakite (this work) and of natural wairakite (Takéuchi *et al.*, 1979), which suggests that four of the six tetrahedral sites are occupied largely by Si and two largely by Al.

It is not possible to perform a unique simulation of the MAS NMR spectrum due to the overlaps between the peaks, the moderate signal-to-noise ratio, and the potentially large number of Si peaks. We anticipate that the majority of the intensity will be in the peaks due to $Q^4(2Al)$ Si in the four sites T11A, T11B, T12A, and T12B. However, if there is any T-site disorder, there could be peaks due to Si in $Q^4(1Al)$ or $Q^4(3Al)$ in any of these four sites, plus $Q^4(1Al)$, $Q^4(2Al)$, or

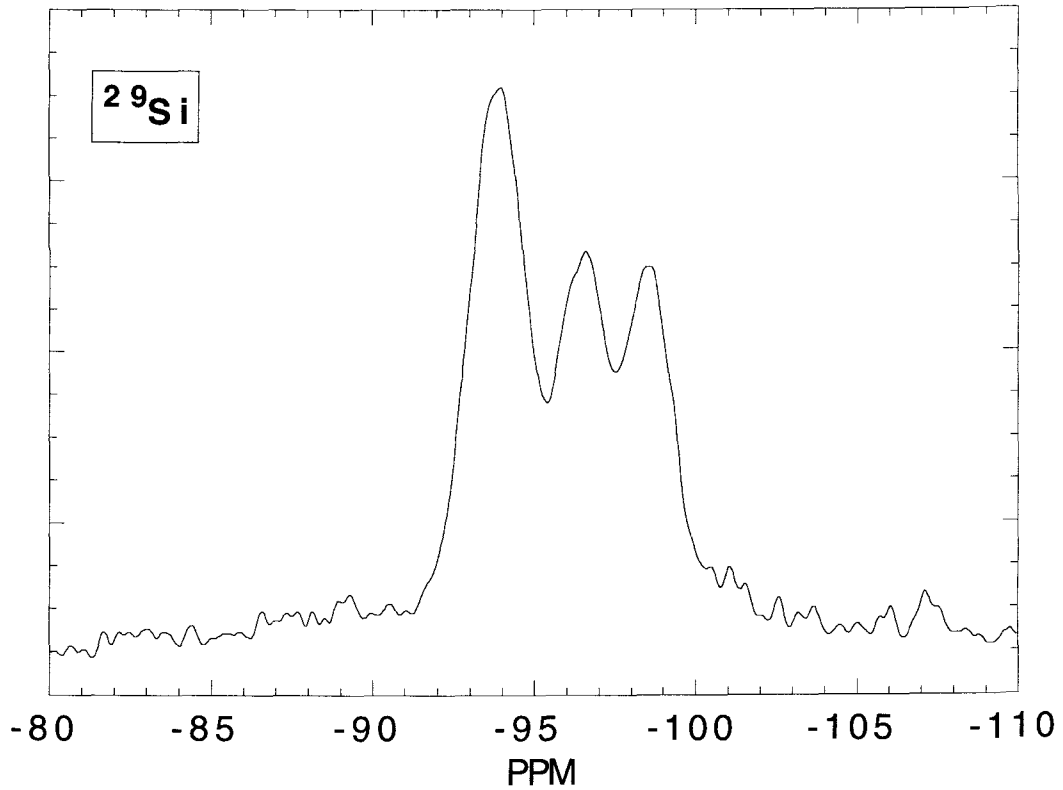

FIG. 3. Single pulse ^{29}Si MAS NMR spectrum for synthetic Ca-wairakite. Note the presence of broad, low intensity shoulders centred at about −89 and −101 ppm on the flanks of the main peaks. The small peak at about −107 ppm is due to a quartz impurity.

Q^4(3Al) in the T2A or T2B sites. In an attempt to circumvent these complications we have fitted the spectrum with five peaks, three of them corresponding to the three main features in the spectrum, plus one at −89 ppm and one at about −101 ppm to fit the shoulders on the high and low frequency sides of the main peaks. About 90% of the total intensity of the spectrum is in the three main peaks and, as suggested from the preliminary integration, the three peaks are in the proportion 2:1:1 within an error of ± 5%. Note that the presence of the two minor peaks (about 10% total intensity) indicates the presence of some disorder and this, in turn, suggests that some of the intensity in these three main peak regions will be due to contributions from other minor Q^4(1Al) and/or Q^4(3Al) sites, and possibly from some Si in T2 sites. We conclude that the main Si intensity is due to four distinct Si Q^4(2Al) sites but that 10–20% of the Si occurs in other sites.

The order of increasing T–O–T angles (Table 2) is T11B = T12A < T12B < T11A. Based on the well known empirical correlation between mean T–O–T angle and ^{29}Si NMR chemical shift, Kohn *et al.* (1997) have recently derived equations relating specifically to Q^4(2Al)Si species. On this basis, we assign the −94 ppm peak to Q^4(2Al) silicons in both T11B and T12A sites, the −96.6 ppm peak to Q^4(2Al) silicons in T12B, and the −98.6 ppm peak to Q^4(2Al) silicons in T11A. The small peaks at −89 and −101 ppm are unlikely to be due to Q^4(2Al) silicons in either of the T2 sites, as these sites both have mean T–O–T angles between those for T12B and T11A. The substitution of Si for Al in the next nearest neighbour (NNN) shell typically changes the ^{29}Si chemical shift by 4–5 ppm (Kirkpatrick *et al.*, 1986), therefore it is likely that the −101 peak is due to T12B(1Al) silicon, and that at −89 ppm might be due to either T11B(3Al)

or T12A(3Al) silicon. The T11B(3Al) possibility is the more likely as the X-ray results indicate that the 3 Al atoms could be distributed over any three of the 4 connected T-sites (T12A, T12B, 2T2A; Table 3), while neither the T11A nor the T11B tetrahedron, which are connected to T12A (Table 3), appear to contain Al.

The presence of significant Al in the T12 sites implies that Si must be present in the T2 sites. Mean T–O–T angles for T2A and T2B (141.3 and 143.5°) should be equivalent to NMR peaks for T2A(2Al) silicons at about −97 ppm and for T2B(2Al) silicons at about −98 ppm. These positions coincide with major peaks from T12B(2Al) and T11A(2Al) silicons therefore the presence of such T2(2Al) silicon sites cannot be confirmed or discounted from the ^{29}Si spectrum.

The ^{27}Al spectra at the two fields are shown in Fig. 4. The spectrum obtained at 14.1 T consists of what appears to be a quadrupolar lineshape over the region 64 ppm to 30 ppm, together with a very small peak at 68 ppm and a peak at 2.5 ppm. The 2.5 ppm peak is due to octahedral Al, and is likely to reflect the presence of an amorphous impurity phase as no crystalline impurity was detected which contains octahedral Al. The peak at 68 ppm is probably a spinning sideband of the 2.5 ppm peak. An attempt to extract values for the shift and quadrupole parameters for Al in wairakite was made by simulating both the high and low field spectra. In principle, the isotropic chemical shifts (δ_i), nuclear quadrupole coupling constants (c_q), and asymmetry parameter (η), of each Al site can be extracted, thus providing abundant structural information. However, in this case it was found that the presence of Al in impurity phases (peaks at around 60 ppm due to anorthite and at 3 ppm probably due to a phase containing octahedral Al)

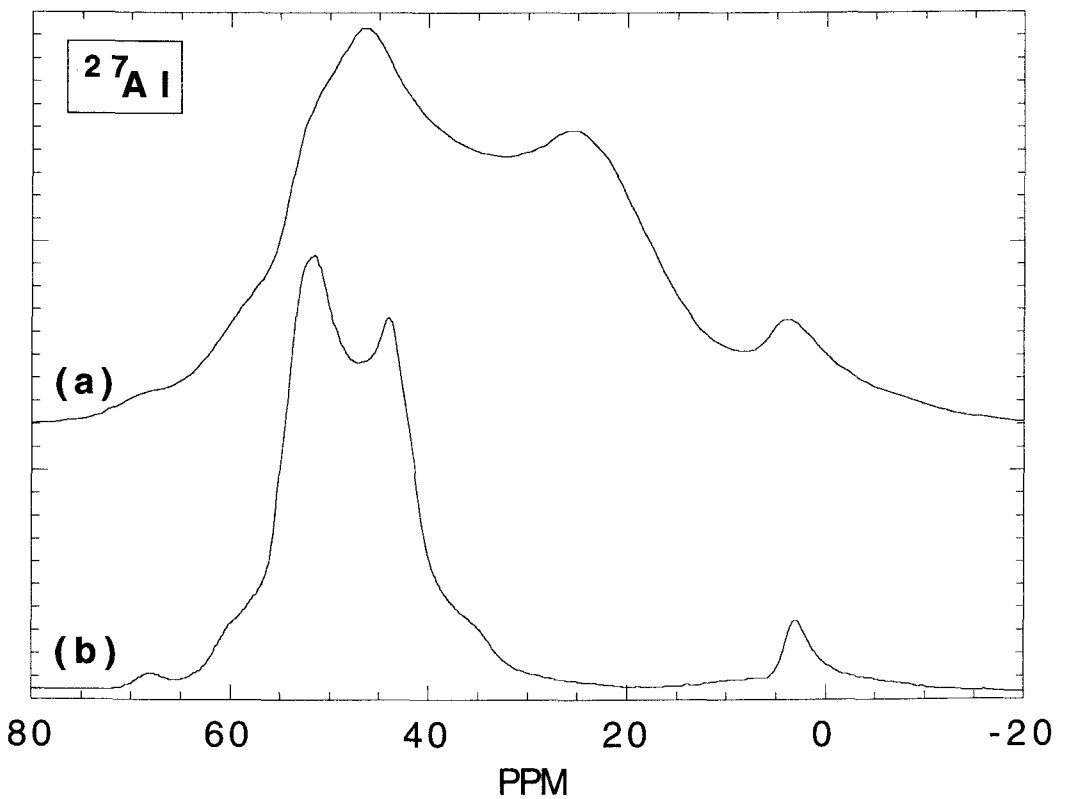

FIG. 4. The ^{27}Al MAS NMR spectra for Ca-wairakite at two magnetic fields of : (*a*) Low field; and (*b*) High field. Impurity peaks are present at about 3 ppm (octahedral Al), 60 ppm (anorthite) and 68 ppm (spinning side band of 3 ppm peak).

and the very similar geometries of the two main Al sites made the simulations somewhat ambiguous. Thus, the spectra could be simulated adequately with just one Al site with δ_i = 57ppm, c_q = 6.1 MHz, η = 0.2, and 400Hz dipolar broadening. The isotropic chemical shift of 57 ppm corresponds to a mean T–O–T bond angle of 150° according to the correlation of Lipmaa *et al.* (1986), or an angle of 145° using the correlation for Si/Al ordered phases in Phillips *et al.* (1989) . These mean T–O–T angle estimates compare with our X-ray structure values of 141.3 and 143.5° for the Al-rich T2A and T2B sites, respectively. The field gradient of 6.1 MHz is consistent with the predictions of Ghose and Tsang (1973) for aluminosilicates, based on the shear strain of the tetrahedra calculated using our atomic coordinates. No information can be extracted regarding the detailed distribution of Al within the framework.

Conclusions and wider implications

Based on the ^{29}Si NMR and powder XRD data it is clear that our synthetic Ca-wairakite is significantly more disordered than the natural sample of Takéuchi *et al.* (1979): this can be correlated with the smaller distortion from the cubic pseudo-cell (*c*/*a* ratio closer to 1.0) for the synthetic sample. The ^{29}Si NMR results for synthetic Ca-wairakite suggest that about 80–90% of the total Si occurs as Q^4(2Al) silicons in the T11A, T11B, T12A and T12B sites, but the possibility that some of these silicons could be present in T2A and T2B sites cannot be assessed because of peak overlap with Q^4(2Al) silicons in T12B and T11A sites, respectively. Small peaks which have been assigned to T12B(1Al) and T11B(3Al) silicons appear to account for about 5% Si in each site. XRD structural information show that about 80% of total Ca is in the M2 site with 10% Ca disordered into each of M12A and M12B, with the M11 sites being vacant. Following the work of Takéuchi *et al.* (1979) regarding the coupling of Ca and Al, we conclude that 80% of total Al is coupled to Ca in M2 and occupies T2 sites, while 20% of the total Al is coupled to Ca in M12 sites and occupies adjacent T12A and T12B tetrahedral sites. By contrast, the M11 site is vacant pointing to the absence of Al in adjacent T11 sites. It follows that the Si displaced from T12 sites must occupy T2, most likely as T2(2Al) type sites. The deductions based on ^{29}Si NMR and on Ca site-ordering data are in line with tetrahedral occupancies deduced from mean T–O bond lengths, except that the T12B–O bond appears to have refined to an anomalously short value.

Liou (1970) described synthesis of tetragonal disordered Ca-wairakite which transformed slowly to the ordered monoclinic form; this transformation was believed to require experiments of at least 1500 hours. The fact that our synthetic monoclinic Ca-wairakite, which was synthesized over a time period of 2184 hours, shows a significant amount of site disorder suggests that Liou's samples might not be fully ordered.

Acknowledgements

We thank the EPSRC for providing synchrotron radiation facilities and R. Dupree (Warwick University) and I. Sadler and D. Reed (Edinburgh University) for NMR facilities.

David Plant kindly made the microprobe analyses of the sample.

References

Aoki, M. and Minato, H. (1980) Lattice constants of wairakite as a function of chemical composition. *Amer. Mineral.*, **65**, 1212–6.

Bayer, G. (1973) Thermal expansion of new leucite-type compounds. *Naturwissenschaften*, **60**, 102–3.

Bell, A.M.T. and Henderson, C.M.B. (1994*a*) Rietveld refinement of dry-synthesized $Rb_2ZnSi_5O_{12}$ leucite by synchrotron X-ray powder diffraction. *Acta Crystallogr.*, **C50**, 984–6.

Bell, A.M.T. and Henderson, C.M.B. (1994*b*) Rietveld refinement of the structures of dry-synthesized $M Fe^{III}Si_2O_6$ leucites (M = K, Rb, Cs) by synchrotron X-ray powder diffraction. *Acta Crystallogr.*, **C50**, 1531–6.

Bell, A.M.T. and Henderson, C.M.B. (1996) Rietveld refinements of the *Pbca* structures of $Rb_2CdSi_5O_{12}$, $Cs_2MnSi_5O_{12}$, $Cs_2CoSi_5O_{12}$ and $Cs_2NiSi_5O_{12}$ leucites by synchrotron X-ray powder diffraction. *Acta Crystallogr.*, **C52**, 2132–9.

Bell, A.M.T., Henderson, C.M.B., Redfern, S.A.T., Cernik, R.J., Champness, P.E., Fitch, A.N. and Kohn, S.C. (1994*a*) Structures of synthetic $K_2MgSi_5O_{12}$ leucites by integrated X-ray powder diffraction, electron diffraction and ^{29}Si MAS NMR methods. *Acta Crystallogr.*, **B50**, 31–41.

Bell, A.M.T., Redfern S.A.T., Henderson, C.M.B. and Kohn, S.C. (1994*b*) Structural relations and tetrahedral ordering pattern of synthetic orthorhombic

$Cs_2CdSi_5O_{12}$ - a combined synchrotron X-ray powder diffraction and multinuclear MAS NMR-study. *Acta Crystallogr.*, **B50**, 560–6.

Bruno, E., Chiari, G. and Facchinelli, A. (1976). Anorthite quenched from 1530°C. I. Structure refinement. *Acta Crystallogr.*, **B32**, 3270–80.

Cernik, R.J., Murray, P.K., Pattison, P. and Fitch, A.N. (1990) A 2-circle powder diffractometer for synchrotron radiation with a closed-loop encoder feedback system. *J. Appl. Crystallogr.*, **23**, 292–6.

Collins, S.P., Cernik, R.J., Pattison, P., Bell, A.M.T. and Fitch, A.N. (1992) A 2-circle powder diffractometer for synchrotron radiation on station 2.3 of the SRS. *Rev. Sci. Instrum.*, **63**, 1013–4.

Coombs, D.S. (1955) X-ray observations on wairakite and non-cubic analcime. *Mineral. Mag.*, **30**, 699–708.

England, K.E.R., Henderson, C.M.B., Charnock, J.M. and Vaughan, D.J. (1994) Investigation of Fe structural environments in 'leucite'-type framework silicates using a combination of Mössbauer and X-ray absorption spectroscopies. *Hyperfine Interactions*, **91**, 709–14.

Faust, G.T. (1963) Phase transitions in synthetic and natural leucite. *Schwiz. Mineral. Petrogr. Mitt.*, **43**, 165–95.

Galli, E., Gottardi, G. and Mazzi, F. (1978) The natural and synthetic phases with the leucite framework. *Mineral. Petrogr. Acta*, **22**, 185–93.

Ghose, S. and Tsang, T. (1973) Structure dependence of quadrupole coupling constant e^2qQ/h for ^{27}Al and crystal field parameter D for Fe^{3+} in aluminosilicates. *Amer. Mineral.*, **58**, 748–55.

Heinrich, A.R. and Baerlocher, Ch. (1991) X-ray Rietveld structure determination of $Cs_2CuSi_5O_{12}$, a pollucite analog. *Acta Crystallogr.*, **C47**, 237–41.

Henderson, C.M.B. (1969) Substitution of Rb, Tl and Cs in K-feldspar. *Progr. Exp. Petrol. (NERC)*, **1**, 53–7.

Henderson, C.M.B. (1984) Feldspathoid stabilities and phase inversions — a review. In *Feldspars and Feldspathoids*. Proc. NATO Advanced Study Institute, D.Reidel, 471–99.

Henderson, C.M.B. and Taylor, D. (1969) An experimental study of the leucite mineral group. *Progr. Exp. Petrol. (NERC)*, **1**, 45–50.

Hogan, M.A. and Risbud, S.H. (1991) Gel-derived amorphous cesium-aluminosilicate powders useful for formation of pollucite glass-ceramics. *J. Materials Res.*, **6**, 217–9.

Jorgensen, J.D. (1978) Compression mechanisms in α-quartz structures — SiO_2 and GeO_2. *J. Appl. Physics*, **49**, 5473–8.

Kirkpatrick, R.J., Dunn, T., Schramm, S., Smith, K.A., Oestrike, R. and Turner, G. (1986) Magic angle spinning NMR spectroscopy of silicate glasses: A review. In *Structure and bonding in non-crystalline solids*. (Eds. G.E. Walfren and A.G. Revesz), pp 303–22. Plenum Press, New York.

Kohn, S.C., Dupree, R., Mortuza, M.G. and Henderson, C.M.B. (1991) An NMR study of structure and ordering in synthetic $K_2MgSi_5O_{12}$, a leucite analogue. *Phys. Chem. Mineral.*, **18**, 144–52.

Kohn, S.C., Henderson, C.M.B. and Dupree, R. (1994) NMR-studies of the leucite analogues $X_2YSi_5O_{12}$, where X = K, Rb, Cs; Y = Mg, Zn, Cd. *Phys. Chem. Mineral.*, **21**, 176–90.

Kohn, S.C., Henderson, C.M.B. and Dupree, R. (1995) Si-Al order in leucite revisited: New information from an analcite-derived analogue. *Amer. Mineral.*, **80**, 705–14.

Kohn, S.C., Henderson, C.M.B. and Dupree, R. (1997) Si/Al ordering in leucite group minerals and ion-exchanged analogues: an MASNMR study. *Amer. Mineral.*, **82**, 1133–40.

Kumar, R., Rakiewicz, E.F. and Rajagopalan, K. (1993) Preparation and characterization of fluid cracking catalysts containing pollucite. *J. Catalysis*, **143**, 304–7.

Lange, R.A., Carmichael, I.S.E. and Stebbins, J.F. (1986) Phase transitions in leucite ($KAlSi_2O_6$), orthorhombic $KAlSiO_4$, and their iron analogues ($KFeSi_2O_6$, $KFeSiO_4$). *Amer. Mineral.*, **71**, 937–45.

Liou, J.G. (1970) Synthesis and stability relations of wairakite, $CaAl_2Si_4O_{12}{\cdot}2H_2O$. *Contrib. Mineral. Petrol.*, **27**, 259–82.

Lipmaa, E., Samoson, A. and Mägi, M. (1986) High resolution ^{27}Al NMR of aluminosilicates. *J. Amer. Chem. Soc.*, **108**, 1730–5.

Loewenstein, W. (1954) The distribution of aluminum in the tetrahedra of silicates and aluminates. *Amer. Mineral.*, **39**, 92–6.

Mackert, J.R., Rueggeberg, F.A., Lockwood, P.E., Evans, A.L. and Thompson, W.O. (1994) Isothermal anneal effect on microcrack density around leucite particles in dental porcelain. *J. Dental Res.*, **73**, 1221–7.

Mazzi, F. and Galli, E. (1978) Is each analcime different? *Amer. Mineral.*, **63**, 448–60.

Mazzi, F., Galli, E. and Gottardi, G. (1976) The crystal structure of tetragonal leucite. *Amer. Mineral.*, **61**, 108–15.

Murdoch, J.B., Stebbins, J.F., Carmichael, I.S.E. and Pines, A. (1988) A ^{29}Si nuclear magnetic resonance study of silicon-aluminum ordering in leucite and analcite. *Phys. Chem. Mineral.*, **15**, 370–82.

Murray, A.D., Cockcroft, J.K. and Fitch, A.N. (1990) Powder Diffraction Program Library (PDPL). Univ. College, University of London.

Nishioka, M., Yanagisawa, K. and Yamasaki, N. (1990) Solidification of sludge ash by hydrothermal hot-pressing. *Research J. Water Pollution Federation*, **62**, 926–32.

Ohmsbredemann, U., Pentinghaus, H. and Heger, G. (1986) Neutron powder diffraction studies of the germanate leucites $KAlGe_2O_6$ $KGaGe_2O_6$ and $CsAlGe_2O_6$. *Z. Kristallogr.*, **174**, 163–5.

Palmer, D.C. and Salje, E.K.H. (1990) Phase-transitions in leucite – dielectric properties and transition mechanism. *Phys. Chem. Min*eral., **17**, 444–52.

Palmer, D.C., Salje, E.K.H. and Schmahl, W.W. (1989) Phase-transitions in leucite – X-ray diffraction studies. *Phys. Chem. Min*eral., **16**, 714–9.

Palmer, D.C., Dove, M.T., Ibberson, R.M. and Powell, B.M. (1997) Structural behaviour, crystal chemistry, and phase transitions in substituted leucite: High-resolution neutron powder diffraction studies. *Amer. Mineral.*, **82**, 16–30.

Peacor, D.R. (1968) A high-temperature single crystal diffractometer study of leucite, (K, Na)$AlSi_2O_6$. *Z. Kristallogr.*, **127**, 213–24.

Pechar, F. (1988) The crystal structure of natural monoclinic analcime ($NaAlSi_2O_6 \cdot H_2O$). *Z. Kristallogr.*, **184**, 63–9.

Phillips, B.L., Kirkpatrick, R.J. and Putnis, A. (1989) Si,Al ordering in leucite by high-resolution ^{27}Al MAS NMR spectroscopy. *Phys. Chem. Mineral.*, **16**, 591–8.

Phillips, B.L., Kirkpatrick, R.J. and Carpenter, M.A. (1992) Investigation of short-range Al,Si order in synthetic anorthite by ^{29}Si MAS NMR spectroscopy. *Amer. Mineral.*, **77**, 484–94.

Redfern, S.A.T. and Henderson, C.M.B. (1996) Monoclinic-orthorhombic phase-transition in the $K_2MgSi_5O_{12}$ leucite analog. *Amer. Mineral.*, **81**, 369–74.

Ren, X., Komarneni, S. and Roy, D.M. (1990) Novel $CsAl_2PO_6$ of pollucite structure – synthesis and characterization. *Mat. Res. Bull.*, **25**, 665–70.

Rietveld, H.M. (1969). A profile refinement method for nuclear and magnetic structures. *J. Appl. Crystallogr.*, **2**, 65–71.

Roedder, E.W. (1951) The system K_2O-MgO-SiO_2. Part 1. *Amer. J. Sci.*, **249**, 81–130.

Steiner, A. (1955) Wairakite, the calcium analogue of analcime, a new zeolite mineral. *Mineral. Mag.*, **30**, 691–8.

Takéuchi, Y., Mazzi, F., Haga, N. and Galli, E. (1979) The crystal structure of wairakite. *Amer. Mineral.*, **64**, 993–1001.

Taylor, D. (1983) The structural behaviour of tetrahedral framework compounds – a review. Part I. Structural behaviour. *Mineral. Mag.*, **47**, 319–26.

Taylor, D. (1984) The structural behaviour of tetrahedral framework compounds – a review. Part II. Framework structures. *Mineral. Mag.*, **1**, 65–79.

Taylor, D. (1991) Thermal-expansion data – 15 – Complex oxides with the leucite structure and frameworks based on 6-membered rings of tetrahedra. *British Ceram. Soc.Trans. J.*, **90**, 197–204.

Taylor, D. and Henderson, C.M.B. (1968) The thermal expansion of the leucite group of minerals. *Amer. Mineral.*, **53**, 1476–89.

Torres-Martinez, L.M. and West, A.R. (1989) Pollucite-related and leucite-related phases – $A_2BX_5O_{12}$ and ACX_2O_6; (A = K, Rb, Cs; B = Be, Mg, Fe, Co, Ni, Cu, Zn, Cd; C = B, Al, Ga, Fe, Cr; X = Si, Ge). *Z. anorg. allg. Chem.*, **573**, 223–30.

Yanagisawa, K., Nishioka, M. and Yamasaki, N. (1987) Immobilization of cesium into pollucite structure by hydrothermal hot-pressing. *J. Nucl. Sci. Tech.*, **24**, 51–60.

[*Manuscript received 8 January 1997: revised 12 August 1997*]